The American Journal of Pathology, Vol. 173, No. 1, July 2008

DOI: 10.2353/ajpath.2008.070732

Tumorigenesis and Neoplastic Progression

C-C Chemokine Receptor 5 on Pulmonary Fibrocytes Facilitates Migration and Promotes Metastasis via Matrix Metalloproteinase 9

Hendrik W. van Deventer,*† Qing Ping Wu,† Daniel T. Bergstralh,‡ Beckley K. Davis,‡ Brian P. O'Connor,‡ Jenny P.-Y. Ting,†‡ and Jonathan S. Serody*†‡

From the Department of Medicine, Division of Hematology/Oncology, the Department of Microbiology and Immunology,‡ and the Lineberger Comprehensive Cancer Center,† University of North Carolina at Chapel Hill, Chapel Hill, North Carolina*

Previously, our group has used a B16-F10 melanoma model to show that C-C chemokine receptor 5 (CCR5) knockout ($CCR5^{-/-}$) mice form fewer pulmonary metastases than wild-type mice. This advantage can be eliminated by injecting $CCR5^{-/-}$ mice with wild-type pulmonary mesenchymal cells before tumor injection. In this article, we present the mechanisms underlying this finding. First, we demonstrate that wild-type mesenchymal cells migrate to CCL4 more efficiently *in vitro* than $CCR5^{-/-}$ cells. Wild-type mesenchymal cells were also 3.6 (1.85 to 5.85) times more efficient than $CCR5^{-/-}$ cells at migrating into the lung after intravenous injection ($P < 0.01$). The injection of wild-type but not $CCR5^{-/-}$ mesenchymal cells led to a 7.0 ± 1.6 ($P < 0.05$)-fold induction of matrix metalloproteinase 9 (MMP9) in the host lung. Neither wild-type nor $CCR5^{-/-}$ cells caused significant increases in MMP2, MMP3, or MMP8. Inhibition of the gelatinase activity of MMP9 decreased the number of metastases and restored the advantage that $CCR5^{-/-}$ mice have over wild-type mice. Further analysis showed that the $CCR5^{+}$ mesenchymal cells expressed $CD45^{+}$ and $CD13^{+}$ but did not express α-smooth muscle actin. This phenotype is characteristic of a subset of mesenchymal cells called fibrocytes. Together, these data suggest a novel role for CCR5 in the migration of pulmonary fibrocytes and the promotion of metastasis. *(Am J Pathol 2008, 173:253–264; DOI: 10.2353/ajpath.2008.070732)*

More than 100 years ago, Stephen Paget suggested that the viability of cancer cells at distant sites is determined by both the cancer cell and the host tissue.[1] His concept of seed and soil has taken on prophetic significance with the understanding of the tumor microenvironment and its contribution to the growth and survival of metastatic cancer cells. More recently, this concept has been refined with the description of the premetastatic niche.[2] In short, the host tissue prepares to accept metastases before the entry of tumor cells into the circulation. According to Kaplan and colleagues,[3] this process is the result of the influx of bone marrow-derived stromal cells. The migration of these stromal cells is mediated in part by chemokines and chemokine receptors. In particular, these authors find that the migration of stromal cells to the lung is promoted by the chemokine CXCL12 and the chemokine receptor CXCR4.[3]

Chemokines are small structurally related molecules whose primary function is the recruitment of hematopoietic cells.[4] These molecules can be classified as homeostatic or inflammatory.[5] CXCL12 is a typical homeostatic chemokine. It is constitutively produced, and it binds to only one chemokine receptor, CXCR4.[6] In contrast, the expression of inflammatory chemokines is induced by inflammatory stimuli. Such chemokines bind multiple receptors, and the receptors bind multiple chemokines.[7] Cell migration is controlled by a combinatorial mix of these chemokines and their receptors. Our study has focused on the role of the inflammatory chemokine receptor C-C chemokine receptor 5 (CCR5) in the tumor microenvironment.

We have observed that CCR5 knockout ($CCR5^{-/-}$) mice develop significantly fewer lung metastases than their wild-type counterparts. The $CCR5^{-/-}$ mice maintained this advantage even after transplantation with wild-type bone marrow. This experiment suggests CCR5 promotes metastasis by its expression on nonhematopoietic stromal cells. This hypothesis was tested by injecting wild-type pulmonary

Supported by the National Cancer Institute (grant CA-89217 to J.S.).

Accepted for publication April 14, 2008.

Address reprint requests to Dr. Hendrik van Deventer, Division of Hematology/Oncology, University of North Carolina at Chapel Hill, Rm 3009 Old Clinic Building, Chapel Hill, NC 27599-7305. E-mail: hvand@med.unc.edu.

mesenchymal cells into CCR5$^{-/-}$ mice before tumor injection. These mesenchymal cells increased the number of metastases equal to the wild-type mice.[8]

Our current study provides the mechanism underlying our previous findings. First, we establish that CCR5 is required for the migration of pulmonary mesenchymal cells into the lung. We go on to show that CCR5 is only expressed on the CD45^{+} mesenchymal cells. This subset has a phenotype consistent with fibrocytes. Lastly, we show that these pulmonary fibrocytes promote metastasis through the induction of matrix metalloproteinase 9 (MMP9) in the host tissue. Thus, we establish a role for the CCR5^{+} pulmonary fibrocyte in the formation of the premetastatic niche.

Materials and Methods

Mice

C57BL/6J wild-type and C57BL/6-Tg (ACTB-EGFP) 1Osb/J enhanced green fluorescent protein transgenic (EGFP-Tg) mice were purchased from Jackson Laboratories (Bar Harbor, ME). Chemokine receptor 5 knockout (CCR5$^{-/-}$) mice have been described previously.[9,10] EGFP-Tg CCR5$^{-/-}$ mice were generated by crossing CCR5$^{-/-}$ mice with EGFP-Tg mice as previously described.[11] All animals had been back crossed at least eight generations and were housed in pathogen-free conditions. All experiments were conducted using protocols approved by Institutional Animal Care and Use Committee of the University of North Carolina at Chapel Hill.

Mesenchymal Cell Isolation

Pulmonary mesenchymal cells were isolated by the method described by Schuler and colleagues[12] with a few modifications. In brief, the lungs were removed, minced, and incubated in digestion media of 2% fetal calf serum/RPMI (Life Technologies, Inc., Carlsbad, CA) with 1 mg/ml of collagenase A and 0.02 mg/ml of DNase I (Boehringer Mannheim, Mannheim, Germany) for 35 minutes at 37°C with continuous rocking. After red cell lysis, the resulting suspension was plated in 10% fetal calf serum/Dulbecco's modified Eagle's medium (Life Technologies, Inc.) and cultured in 37°C with 5% CO_2. The media was replaced after 1 hour and every 3 to 4 days thereafter. Cells were split 3:1 at 70 to 80% confluence. Only cells from the second or third passage were used in experiments. *In vitro* mesenchymal cells were viewed by phase microscopy using an Olympus 1 × 70 inverted microscope (Olympus America, Inc., Melville, NY). Images were captured with an Olympus QColor3 camera and QCpture 2.56 software.

Flow Cytometry

Flow cytometry analysis was applied to mesenchymal cells in culture and single cell lung suspensions. Nonspecific binding was blocked with anti-CD16/CD32 (BD Biosciences Pharmingen, San Diego, CA) and 3% fetal calf serum. The samples were incubated with the following antibodies: anti-MHC Class II (AF6-120.1), anti-CD14 (rmC5-3), anti-CD 45 (31-F11), anti-CCR5 (C34-3448) (all Pharmingen), anti-CD 13 (R3-63), anti-CD34 (MEC14.7) (AbD Serotec, Oxford, UK), anti-F4/80 (C1: A3-1) (Cedarlane, Burlington, Canada), or anti-Thy1.1 (OX-70) (Abcam, Cambridge, MA). Bone marrow and spleen cells were used as positive controls. Data were collected on a FACSCalibur (BD Biosciences, San Jose, CA) and analyzed using WinMDI version 2.8 software (Scripps Research Institute, La Jolla, CA).

Mesenchymal cell survival was tested by growing cells to 70% confluency in six-well plates. At that point, the wells were washed with phosphate-buffered saline (PBS); and the cells were grown in serum-free media alone or with CCL4 (50 ng/ml) or CCL5 (5 ng/ml) (Peprotech Inc., Rocky Hill, NJ). After 24 or 48 hours, the cells were harvested and stained with annexin V and 7-AAD (Invitrogen, Carlsbad, CA) according to the manufacturer's instructions. Results are expressed as the percentage of annexin V-positive cells after excluding 7-AAD^{+}, annexin V^{-} cells.

Semiquantitative and Real-Time Reverse Transcriptase-Polymerase Chain Reaction (RT-PCR)

Total RNA was isolated from pulmonary mesenchymal cells using the RNeasy Plus mini kit (Qiagen, Valencia, CA) according to the manufacturer's protocol. cDNA was synthesized using M-MLV reverse transcriptase (Invitrogen) and random hexamers. RT-PCR was performed using ChromaTaq DNA polymerase (Denville Scientific, Metuchen, NJ) and a Mastercycler thermocycler (Eppendorf, Westbury, NY) with an annealing temperature of 56°C. Primer sequences and cycle number are given in Table 1. The RT-PCR products were visualized using a 1.5% agarose gel; images were taken with the Gel Logic 200 imaging system and processed with Kodak 1D software (Kodak, New Haven, CT).

Real-time RT-PCR was performed using SYBR green and an ABI Prism 7900 real-time RT-PCR system (Applied Biosystems, Foster City, CA). The efficiency of each primer pair was tested against serial dilutions of an amplicon-containing plasmid and the sample. Transcript copy number was normalized against the absolute mRNA amount as measured by the Qubit quantitation platform (Invitrogen). In experiments in which the absolute mRNA was less than 10 ng, samples were normalized by expression of succinate dehydrogenase complex, subunit A, flavoprotein (SDHA). SDHA was used as a housekeeping gene because transcript copy number in the mesenchymal cells had a high degree of correlation with the amount of mRNA in a wide variety of culture conditions.

Immunohistochemistry

In vitro immunohistochemistry was performed by culturing mesenchymal cells in Lab-Tek chamber slides (Nalge Nunc International, Rochester, NY). These cells were

Table 1. Primers Used for Semiquantitative and Real-Time RT-PCR

Gene	Primers (forward, reverse)	Amplicon size	Cycles
CCR5	5′-GAGGTGAGACATCCGTTCC 5′-GACCATCATGTTACCCACAAAACC	205	28
αSMA	5′-ACTGGTATTGTGCTGGACTCT 5′-CGGCAGTAGTCACGAAGGAAT	169	26
SDHA	5′-GGAACACTCCAAAAACAGACCT 5′-CCACCACTGGGTATTGAGTAGAA	105	26
MMP2	5′-CCTGATGTCCAGCAAGTAGATG 5′-AGGAGTCTGCGATGAGCTTA	142	
MMP3	5′-GCACGAGGAGCTAGCAGGTTAT 5′-TGGCAGCATCGATCTTCTTCAC	80	
MMP8	5′-AACCAGGCCAAGGTATTGGA 5′-TTCATGAGCAGCCACGAGAA	101	
MMP9	5′-TGTGCGACCACATCGAACTT 5′-GGCACGCTGGAATGATCTAA	128	

fixed with 4% formalin and permeabilized with 0.2% Triton X-100 (Sigma-Aldrich, St. Louis, MO). Antibodies for α-smooth muscle actin (α-SMA) (1A4) or isotype control (Lab Vision, Fremont, CA) were added at 1:100 after blocking with 10% goat serum. The antibody was detected with an anti-mouse Ig antibody conjugated to Alexa 488 (Invitrogen). Images were captured using Olympus B201 florescent microscope with camera (Olympus, Center Valley, PA).

Western Blotting

Western blotting was performed as previously described.[13] In brief, mesenchymal cells were transferred to six-well plates and cultured in serum-free media overnight. The following day, the cells were treated with CCL4; and cell lysates were harvested. The samples were run on a 10% sodium dodecyl sulfate gel before transfer to nitrocellulose. Phospho-Erk was detected using an antibody from Cell Signaling (Danvers, MA) diluted 1:1000. The secondary antibody was diluted 1:10,000. Western blotting was also applied to lysates of mesenchymal cells sorted by CD45 and Thy1.1. Antibodies for α-SMA (1A4) (Lab Vision) and CCR5 (C34-3448) (Pharmingen) were also diluted 1:1000. Detection of β-actin (H-196) (Santa Cruz Biotechnology, Santa Cruz, CA) was used as a loading control.

Migration Assay

Mesenchymal cells were cultured in serum-free conditions overnight. Approximately 300 μl of serum-free media with and without CCL4 was added to the wells of a 5.7-mm diameter, 300-μl, 96-well ChemoTx plate (Neuroprobe, Gaithersburg, MD). Fifty μl with 5×10^5 wild-type or CCR5$^{-/-}$ mesenchymal cells were added to the filter. Chemokinesis was ruled out by adding CCL4 along with the cells in selected wells. The plate was allowed to incubate for 6 to 8 hours. Nonmigrating cells were then removed with a rubber policeman. The filter was washed with PBS and fixed with 4% paraformaldehyde. Nuclei on the reverse side of the filter were counted after staining with Vectashield with 4,6-diamidino-2-phenylindole (Vector Laboratories, Burlingame, CA). At least 30 high-powered fields were examined per well by an investigator blinded to the treatment. Results are expressed as nuclei per high-powered field.

In Vivo *Experiments*

Details for the melanoma metastasis model have been previously described.[8] In brief, 7.5×10^5 B16 F10 melanoma cells (American Type Culture Collection, Rockville, MD) in 200 μl of PBS were injected via the tail vein. Mice were euthanized 14 days later, and metastases were counted after insufflation with Fekete's destaining solution.[14] Reflected light images of the lung were taken using the SteREO Lumar V12 scope and Axiovision software (Zeiss Microscope Corporation, Thornwood, NY).

To assess migration of mesenchymal cells *in vivo*, cells were isolated from wild-type and CCR5$^{-/-}$ EGFP-Tg mice. Of these EGFP expressing cells 4×10^5 were suspended in 300 μl of PBS and injected via the tail vein. At days 1 and 5, a single cell suspension was formed from the right lung and analyzed by flow cytometry. Forward and side scatter gates were based on cultured mesenchymal cells before the injection. EGFP-Tg gate (FL1) was set to exclude all cells from the lung of an uninjected wild-type mouse. The data were reported as the number of total cells multiplied by the percentage of EGFP-Tg cells. The left lung was washed in cold PBS and viewed with a SteREO Lumar V12 fluorescent microscope and images were captured with Axiovision software (Zeiss). In certain experiments, the above gating strategy was used to sort single cell suspensions by EFGP expression using a MoFlo cytometer (Cytomation, Fort Collins, CO).

Gelatinase inhibitor experiments were performed by dissolving 1 mg of the cyclic peptide CTTHWGFTLC (CTT) or the control peptide STTHWGFTLS (STT) (BioMol, Plymouth Meeting, PA) in 1.5 ml of PBS. This solution was added to an equal volume of mesenchymal cells at a concentration of 2.67×10^6 cells/ml. The resulting mixture was allowed to warm to 37°C before the injection. A 300-μl injection resulted in a dose of 4×10^5 mesenchymal cells with 100 μg of CTT or STT. Migration of mesenchymal cells and the effect on metastasis was measured as described above.

Microarray Analysis

Raw mRNA expression data were generated from the experiments of Altemeier and colleagues[15] and downloaded from European Bioinformatics Institute, Heidelberg, Germany (accession: E-GEOD-2411; *http://www.ebi.ac.uk/microarray*). In these experiments, six mice were given 5 ng/g body weight of lipopolysaccharide by aspiration; and six were given PBS only as a control. Total RNA was harvested 4 to 6 hours later and hybridized onto separate Affymetrix GeneChips Mouse Genome 430A 2.0. Raw data were normalized using an index of SDHA, GAPDH, PyrCarbMur-1, and actin.

Statistics

Unless otherwise stated, data are presented as the mean of measurements taken from three or more separate experiments. Statistical error for these means is presented as ±1 SEM. Confidence intervals were determined using a 60% trimmed mean. *P* values were determined by Mann-Whitney test,[16] and values <0.05 were considered significant. The Bonferroni correction was applied to the microarray experiments.

Results

Mesenchymal Cells Isolated from the Lungs of Wild-Type and CCR5 Knockout Mice Are Phenotypically Similar

In our previous work, we increased the number of metastases in CCR5$^{-/-}$ mice by injecting them with pulmonary mesenchymal cells from wild-type mice. These mesenchymal cells were isolated by culturing a suspension of lung cells in 10% Dulbecco's modified Eagle's medium. Because mesenchymal cells isolated from CCR5$^{-/-}$ lungs did not increase metastasis, we began this investigation by comparing mesenchymal cells from wild-type and CCR5$^{-/-}$ mice.

Pulmonary mesenchymal cells from wild-type and CCR5$^{-/-}$ mice cells were microscopically similar. Each population had pleomorphic appearance with cells ranging from spindle shaped to large and flat (Figure 1A). This microscopic equivalence was corroborated by flow cytometry, which showed similar forward and side scatter profiles of the mesenchymal cells from both mice (Figure 1B). Wild-type and CCR5$^{-/-}$ pulmonary mesenchymal cells were also composed of similar subpopulations as defined by CD45 expression. The CD45^{+} subpopulation from both mice expressed CD13 but not CD14, CD34, CD86, or MHC class II (Figure 1C). Furthermore, no difference was found in the size of this subpopulation ($P = 0.38$).

Wild-type and CCR5$^{-/-}$ mesenchymal cells also had similar CD45-negative cell subpopulations. Neither wild-type nor CCR5$^{-/-}$ CD45^{-} cells expressed CD13, CD34, CD86, and MHC class II. These cells could be separated into two subpopulations by Thy1.1.[17] However, the size of

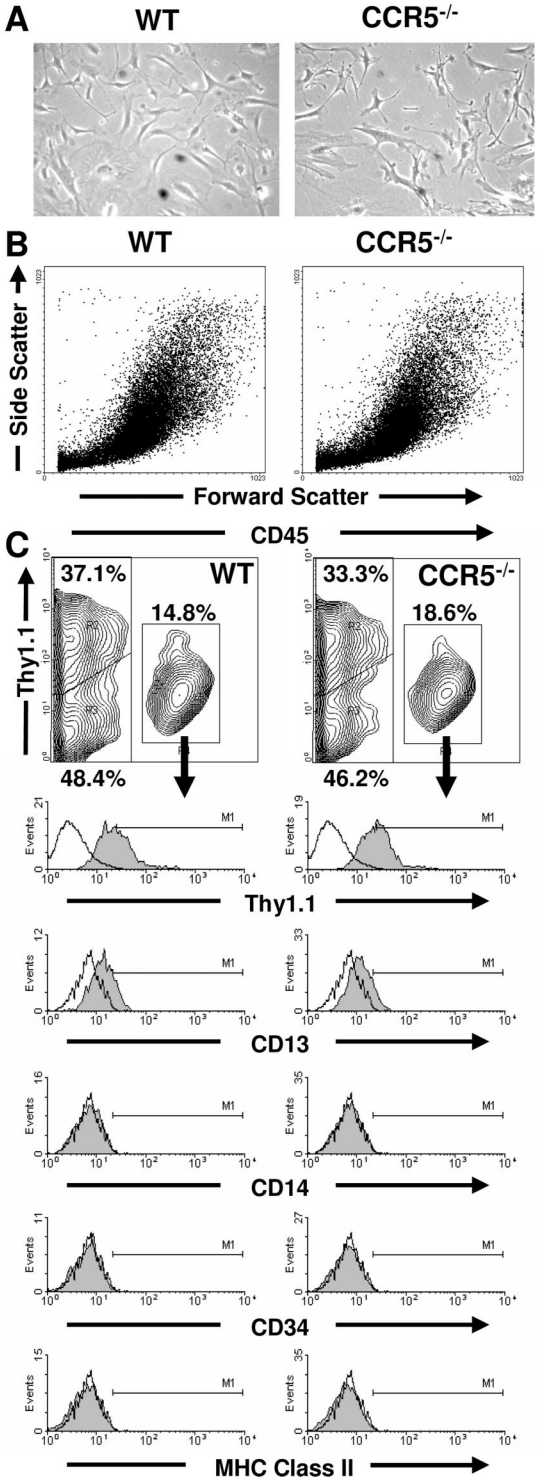

Figure 1. Wild-type and CCR5$^{-/-}$ pulmonary mesenchymal cells are phenotypically similar. **A:** Phase contrast microscopy of wild-type and CCR5$^{-/-}$ mesenchymal cells. **B:** Forward and side scatter patterns of ungated wild-type and CCR5$^{-/-}$ mesenchymal cells by flow cytometry. **C:** Contour graphs of CD45 (*x* axis) and Thy1.1 (*y* axis) expression on wild-type and CCR5$^{-/-}$ mesenchymal cells as measured by flow cytometry. The percentage for each gate is based on the mean of six samples. Single color histograms for CD45^{+} mesenchymal cells are given below each contour graph. These are representative graphs from the six samples. Original magnifications, ×100.

Thy1.1^{+} and Thy1.1^{-} subpopulations were similar in the wild-type and CCR5$^{-/-}$ mice ($P = 0.89$ and $P = 0.66$, respectively). Taken together, neither CD45 nor Thy1.1 expression can explain differences in metastasis after injection into CCR5$^{-/-}$ mice.

Flow cytometry analysis was also used to detect contaminating macrophages by measuring CD11c, CD14, and F4/80. Less than 2% of wild-type and CCR5$^{-/-}$ cells expressed CD11c and CD14, and less than 5% of cells expressed F4/80. No statistical differences were found between the wild-type and CCR5$^{-/-}$ mice. It is highly unlikely that macrophages were experimentally significant because injection of wild-type macrophages did not increase metastasis in CCR5$^{-/-}$ mice (data not shown).

Pulmonary Mesenchymal Cells from Wild-Type and CCR5$^{-/-}$ Mice Show No Difference in Activation or Survival in Vitro

Given the similar cell surface phenotypes of the wild-type and CCR5$^{-/-}$ mesenchymal cells, we examined differences in activation by measuring α-SMA. α-SMA is a marker of myofibroblasts, which has been associated with tumor progression.[18,19] Immunohistochemical staining for α-SMA was similar in the wild-type and CCR5$^{-/-}$ cells (Figure 2A). This observation was corroborated by semiquantitative RT-PCR (Figure 2C). Therefore, the ability of wild-type cells to promote metastasis could not be explained by differences in α-SMA expression.

Differences in metastasis could possibly be explained by differences in survival of wild-type and CCR5$^{-/-}$ mesenchymal cells. We tested this hypothesis by culturing wild-type and CCR5$^{-/-}$ cells in serum-free conditions for 24 to 48 hours. The CCR5 agonists CCL4 and CCL5 were added to final concentrations of 50 and 5 ng/ml, respectively. Using Annexin V as a marker of cell death, we found the average survival in all conditions was 89.8 ± 1.2% for wild-type cells and 89.8 ± 0.% for CCR5$^{-/-}$ cells. There were no significant differences between wild-type and CCR5$^{-/-}$ cells in any conditions (Figure 2B).

Wild-Type Pulmonary Mesenchymal Cells Respond to CCL4 in Vitro

Having established morphological similarities between wild-type and CCR5$^{-/-}$ pulmonary mesenchymal cells, we turned our attention to the function of CCR5. First, we verified the expression of CCR5 by semiquantitative RT-PCR (Figure 2D). Surface expression was confirmed by flow cytometry analysis (see Figure 5A). Both methods demonstrated the presence of CCR5. Next, we tested the ability of CCR5 to induce a downstream signal by measuring activation of the MAP kinase pathway after stimulation with CCL4.[20] MAP kinase activation was detected by Western blotting for phospho-ERK at 30, 60, and 120 minutes after adding CCL4 (Figure 2E). We verified the function of MAPK signal transduction by comparing the chemotaxis of wild-type and CCR5$^{-/-}$ pulmonary mesenchymal cells. Wild-type cells migrated toward CCL4 at concentrations of 25 and 50 ng/ml (Figure 2F). No significant chemotaxis was seen using concentrations of 0 or 100 ng/ml of CCL4. Thus, wild-type mesenchymal cells demonstrated a dose response similar to hematopoietic

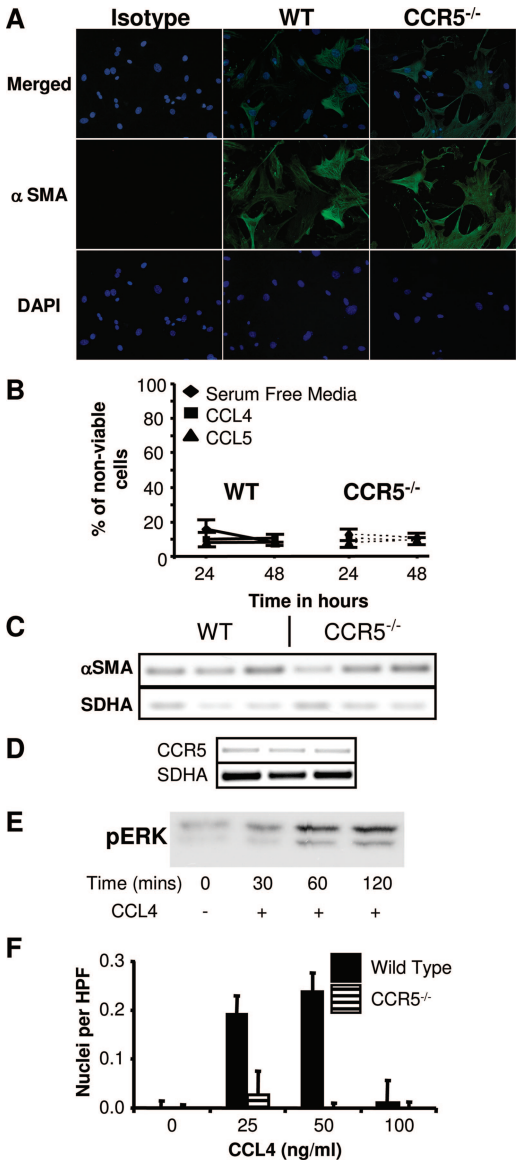

Figure 2. Wild-type pulmonary mesenchymal cells differ from CCR5$^{-/-}$ by their response to CCL4. **A:** Fluorescent microscopy of wild-type and CCR5$^{-/-}$ mesenchymal cells revealing similar staining for α-SMA. **B:** Measurement of cell death by annexin V staining demonstrating no difference in survival of wild-type and CCR5$^{-/-}$ cells. Samples were tested in serum-free media alone or with CCL4 (50 ng/ml) or CCL5 (5 ng/ml). Cell debris was excluded with 7-AAD ($n = 4$). **C:** Semiquantitative RT-PCR demonstrating the presence of α-SMA in wild-type and CCR5$^{-/-}$ mesenchymal cells. The gel shows cDNA from three separate experiments. The number of cycles for each reaction was chosen to assure linear amplification of the transcript. SDHA was chosen as a loading control based on its high degree of correlation with the amount of mRNA in a wide variety of conditions. **D:** Semiquantitative RT-PCR demonstrating the expression of CCR5 in wild-type pulmonary mesenchymal cells ($n = 3$). **E:** Western blotting for phospho-ERK showing a response to CCL4 (50 ng/ml) in wild-type mesenchymal cells. **F:** Chemotaxis assay establishing migration of wild-type but not CCR5$^{-/-}$ mesenchymal cells to CCL4. Cells were added to a 5.7-μm chemotaxis plate and incubated for 6 to 8 hours with varying concentrations of CCL4. Migrating cells were detected on the reverse side of the filter using fluorescent microscopy after fixation and staining with 4,6-diamidino-2-phenylindole. Thirty or more high-powered fields were counted ($n = 3$). Original magnification, ×100.

cells. No such response was seen in CCR5$^{-/-}$ mesenchymal cells.

Wild-Type Mesenchymal Cells Migrate More Efficiently than CCR5$^{-/-}$ Cells in Vivo

We tested the relevance of this *in vitro* chemotaxis by comparing the migration of wild-type and CCR5$^{-/-}$ mesenchymal cells into the lung. This comparison was accomplished by isolating pulmonary mesenchymal cells from wild-type and CCR5$^{-/-}$ EGFP-Tg mice and then injecting 4×10^5 of these cells into the tail vein of wild-type or CCR5$^{-/-}$ mice. Twenty-four hours later, a single cell suspension was formed from the lung and analyzed by flow cytometry. Given the low number of injected cells, flow cytometry gates were set to exclude cells from uninjected control mice (Figure 3A). This gating strategy detected >95% of EGFP-Tg mesenchymal cells taken directly from culture. Furthermore, EGFP-Tg wild-type and EGFP-Tg CCR5$^{-/-}$ cells had similar EGFP fluorescent intensity (Figure 3B).

Using this strategy, we found that wild-type mesenchymal cells were 3.6 (1.85 to 5.85) times more efficient in their ability to migrate into the lung than CCR5$^{-/-}$ cells ($P < 0.003$) (Figure 3C and Table 2). The migratory capacity of wild-type cells did not depend on the presence of CCR5 in the recipient. Equivalent numbers of wild-type EGFP-Tg cells were detected in wild-type and CCR5$^{-/-}$ recipients. These results were confirmed by fluorescent stereomicroscopy (Figure 3E).

We established the kinetics of mesenchymal cell migration by measuring the number of EGFP-Tg cells 5 days after injection. In these experiments, mice were injected with B16-F10 tumor cells 1 day after mesenchymal cell injection. These experiments showed a decrease of 84.7% (72.0 to 96.4%) in the recoverable number of mesenchymal cells ($P < 0.007$) (Figure 3D). In other words, wild-type pulmonary mesenchymal cells were found 1 day after injection, but they did not persist in the lung throughout the long term.

MMP9 Expression Is Induced in Mesenchymal and Host Cells

These results established the presence of wild-type mesenchymal cells in the lungs of CCR5$^{-/-}$ mice at the time that the B16-F10 melanoma cells are injected. The next question was how such a small number of these CCR5 expressing mesenchymal cells can promote metastasis. Stimulation of CCR5 has been linked to the production of MMP9 in a mouse model of emphysema.[21] Because MMP9 has also been correlated with metastasis in melanoma,[22] we used real-time RT-PCR to measure the expression of MMP9 in the EGFP-Tg mesenchymal cells isolated 24 hours after intravenous injection. We found that transcription of MMP9 increased by 6.3 ± 2.2-fold when compared to uninjected mesenchymal cells ($P < 0.05$). In contrast, MMP2 and MMP3 transcripts fell below detection by real-time RT-PCR indicating down-regulation of these genes after injection into CCR5$^{-/-}$ mice (Figure 4A). Transcription of MMP8 was not significantly changed by injection. Data for CCR5$^{-/-}$ EGFP-Tg mesenchymal cells was not included because the number of recovered cells was too small for reliable measurement.

We also measured changes in MMP transcription in the EGFP$^-$ host cells after injection with mesenchymal cells. The transcription of MMP9 was significantly increased (7.0 ± 1.6, $P < 0.05$) in the host after the injection of wild-type mesenchymal cells (Figure 4A). Injection with CCR5$^{-/-}$ mesenchymal cells led to a small increase in MMP9 (2.4 ± 0.5, NS); however, this change was not statistically significant. Transcription of MMP2, MMP3, and MMP8 did not significantly change in the host cells after injection with wild-type or CCR5$^{-/-}$ mesenchymal cells.

Inhibition of Gelatinase Activity Suppresses the Ability of Wild-Type Mesenchymal Cells to Increase Metastasis in CCR5$^{-/-}$ Mice

Next, we determined if this increase in MMP9 transcription contributed to the ability of wild-type mesenchymal cells to promote metastasis. In these experiments, MMP9 activity was inhibited with the addition of gelatinase peptide inhibitor CTTHWGFTLC (CTT).[23,24] Treatment with the altered peptide STTHWGFTLS (STT) was used as the control. In each experiment the peptide and the cells were combined and warmed to body temperature before injection. In Figure 4B, we demonstrated that treatment with CTT had no affect on the migration of wild-type mesenchymal cells into CCR5$^{-/-}$ mice. Therefore, differences in metastases between CTT- and STT-treated mice were not attributable to the inability of CTT-treated cells to migrate into the lung. However, CTT did inhibit the ability of wild-type mesenchymal cells to promote metastasis (Figure 4, C and D). CCR5$^{-/-}$ mice injected with STT (control)-treated wild-type mesenchymal cells developed 50.6% more metastases than CCR5$^{-/-}$ mice injected with CTT-treated cells (116.5 ± 12.3 versus 77.3 ± 9.1, $P < 0.05$). CCR5$^{-/-}$ mice injected with CTT-treated wild-type mesenchymal cells developed the same number of metastases as CCR5$^{-/-}$ mice injected with CCR5$^{-/-}$ cells (77.3 ± 9.1 versus 81.0 ± 7.2, NS).

Wild-Type Pulmonary Fibrocytes Promote Metastasis in CCR5$^{-/-}$ Mice

The experiments discussed thus far have used unsorted pulmonary mesenchymal cells. To better understand the properties of these cells, we sorted these cells using CD45 and Thy1.1 expression. Of the three subpopulations, only the CD45$^+$ population expressed CCR5 (Figure 5A). Furthermore, the CD45$^+$ cells did not express α-SMA (Figure 5B). Taken together, the CD45$^+$ cells were phenotypically similar to fibrocytes.

CD45$^+$ fibrocytes also differed from CD45$^-$ fibroblasts in MMP expression. When compared to the unsorted mesenchymal cell population, the CD45$^-$ cells ex-

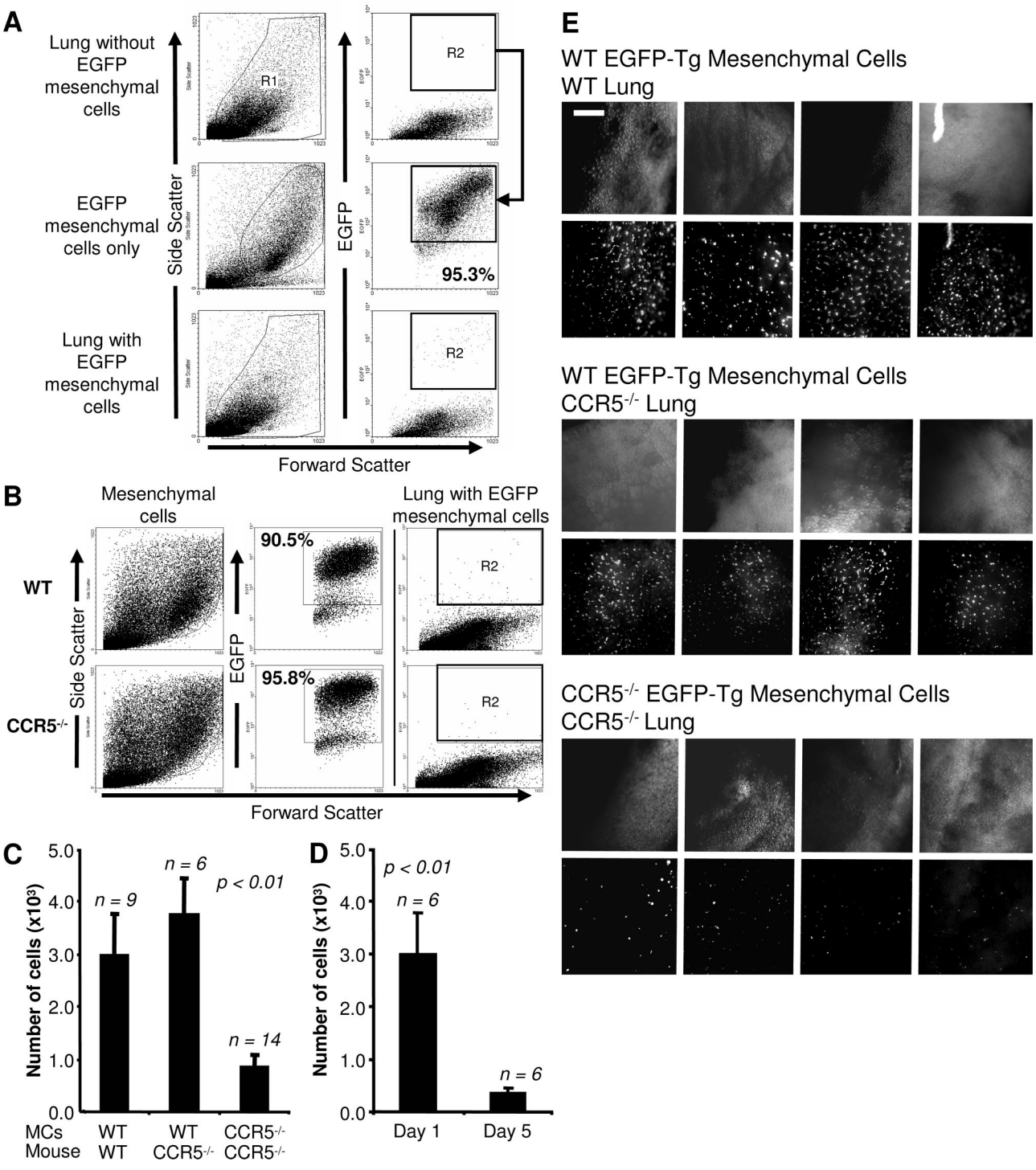

Figure 3. Wild-type mesenchymal cells migrate more efficiently *in vivo* than CCR5$^{-/-}$ cells. **A:** Gating strategy for the detection of injected EGFP-Tg mesenchymal cells. R1 includes viable cells based on FSC/SSC. R2 excludes all EGFP-Tg-negative cells based on flow cytometry analysis of an uninjected lung. These gates detect more than 95% of all EGFP-Tg cells before injection (**middle**). Migrating mesenchymal cells are detected in R2 after injection (**bottom**). **B:** Expression of EGFP-Tg is equivalent in wild-type and CCR5$^{-/-}$ mesenchymal cells. Representative FSC/SSC and FSC/EGFP-Tg dot plots of wild-type and CCR5$^{-/-}$ EGFP-Tg mesenchymal cells. **C:** More wild-type than CCR5$^{-/-}$ cells are detected 24 hours after intravenous injection. Bar graphs show the number of EGFP-Tg cells recovered from the right lung as determined by the percentage of EGFP-Tg cells times the number of cells isolated. The number of animals for each experiment is given above the graph. **D:** The number of detected wild-type fibroblasts decreases throughout time. A similar strategy as described in **C** was applied to mice 1 and 5 days after injection. **E:** Fluorescent microscopic images of the left lungs of mice from **C** using a SteREO Lumar V dissecting scope. Scale bar = 1 mm. Original magnifications, ×42.

Table 2. $EGFP^+$ Mesenchymal Cells Detected by Flow Cytometry

Pulmonary mesenchymal cell	Host	Cells harvested ($\times 10^6$)	Cells analyzed	Events	% EGFP-Tg cells	EGFP-Tg cells ($\times 10^3$)
WT EGFP-Tg	WT (day 1)	7.4 ± 0.49	69,000 ± 4100	28 ± 3	0.04 ± 0.007%	3.0 ± 0.77
WT EGFP-Tg WT	$CCR5^{-/-}$ (day 1)	8.4 ± 1.3	90,000 ± 700	40 ± 4	0.04 ± 0.002%	3.8 ± 0.69
$CCR5^{-/-}$ EGFP-Tg	$CCR5^{-/-}$ (day 1)	6.9 ± 0.48	87,000 ± 7300	10 ± 1	0.01 ± 0.003%	0.9 ± 0.21
WT EGFP-Tg	$CCR5^{-/-}$ (day 5)	6.8 ± 0.66	47,000 ± 3100	3 ± 1	0.01 ± 0.001%	0.4 ± 0.09

pressed MMP2 1.8 ± 0.9 times higher and MMP3 2.1 ± 0.55 times higher than the unsorted population. MMP9 was not detected. On the other hand, $CD45^+$ fibrocytes expressed MMP8 at 3.3 ± 0.48 times higher and MMP9 at 5.1 ± 0.68 times higher than the unsorted mesenchymal cells. MMP2 and MMP3 were not detected (Figure 5C). This pattern of high MMP9 and MMP8 with low MMP2 and MMP3 was similar to that seen in the $EGFP^+$ cells after injection into a $CCR5^{-/-}$ mouse (Figure 4A).

These observations suggested that the increase in MMP9 in the EGFP-Tg mesenchymal cells was not attributable to an induction of MMP9. Instead, this increase was attributable to a selection of $CCR5^+$ fibrocytes. This assertion was further strengthened by the observation that the addition of CCL4 or CCL5 to the pulmonary mesenchymal cells did not lead to an increase in MMP9 (Figure 5D) Therefore, we concluded that the metastasis-producing properties of these fibrocytes was their ability to induce MMP9 in the host tissue.

CCR5 Ligands Are Expressed in the Lung

We identified the CCR5 agonists in an unmanipulated mouse lung using a data mining approach. Raw mRNA expression data from wild-type B6 mice were downloaded from the European Bioinformatics Institute (see Materials and Methods) and normalized to an index of 10 probes.[15] We considered a gene to be detectable if the normalized mRNA value was >0.2. This value was approximately equivalent to a raw expression value of 300. Using the above criteria, we were able to detect 15 of 32 chemokines (Table 3). This set included the CCR5 ligands CCL4, CCL5, and CCL8. Ligands for other fibrocyte-associated chemokine receptors were also present including CCR1 (CCL6, CCL5, CCL9), CCR2 (CCL8), CCR7 (CCL21, CCL19), CXCR1 (CXCL7, CXCL16), CXCR3 (CXCL4, CXCL10), and CXCR4 (CXCL12). Only ligands for CCR3 and CCR9 were absent in the unstimulated lung. We compared the baseline chemokine expression pattern to chemokine expression after the mice had been challenged with lipopolysaccharide. This analysis revealed seven additional detectable chemokines. Three of these seven are ligands for fibrocyte-associated chemokine receptors: CCL22 (CCR4), CCL2 (CCR2), and CCL3 (CCR1, CCR5). Of the CCR5 ligands, three had significant fold increases of mRNA expression including CCL3 (6.8 ± 1.6), CCL4 (2.4 ± 0.3), and CCL5 (2.7 ± 0.4).

Discussion

For this study, we have altered the premetastatic stroma of the lungs of $CCR5^{-/-}$ mice by injecting them with

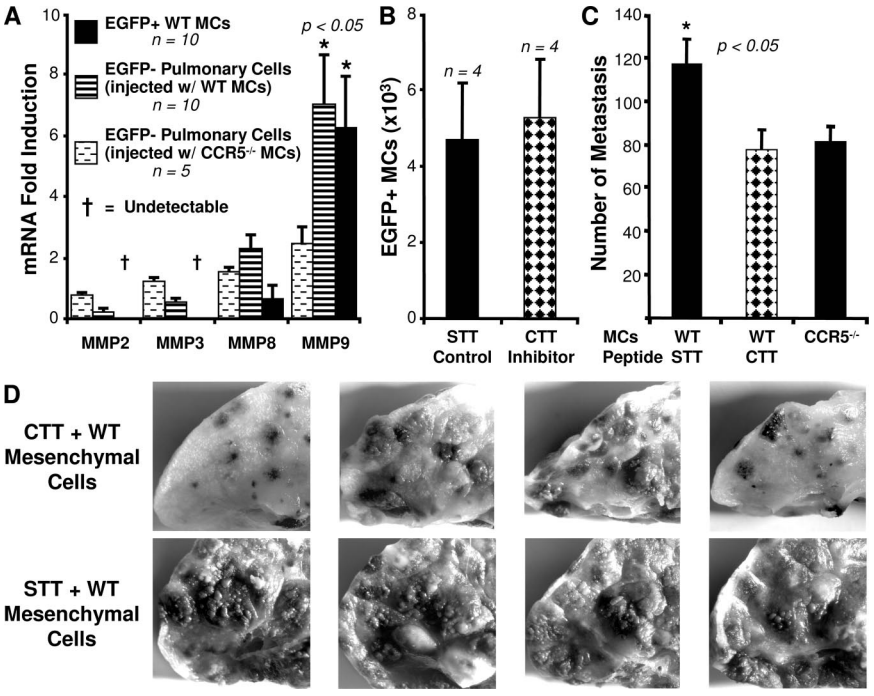

Figure 4. Inhibition of MMP9 blocks the ability of wild-type mesenchymal cells to promote metastasis in $CCR5^{-/-}$ mice. **A:** Transcription of MMP9 increases in migrating mesenchymal cells and host tissue. EGFP-Tg wild-type and $CCR5^{-/-}$ cells were injected into $CCR5^{-/-}$ mice. Twenty-four hours later, EGFP-Tg and non-EGFP-Tg cells were sorted; and mRNA was isolated from each group. Real-time RT-PCR was used to measure the ratio of MMP transcripts from EGFP-Tg cells before and after injection. Copy number was normalized to SDHA. Non-EGFP-Tg cells were compared to an average of sorted cells from six noninjected $CCR5^{-/-}$ lungs. The sample of $CCR5^{-/-}$ EGFP-Tg cells was not included (see text). **B:** Inhibition of gelatinase activity does not affect the migration of wild-type fibroblasts. The bar graph shows the number of wild-type EGFP-Tg mesenchymal cells isolated after injection. The black bar is the number of cells treated with the gelatinase inhibitor CTT; the hatched bar is the number of cells treated with the control peptide STT. **C:** Inhibition of gelatinase results in fewer metastases in $CCR5^{-/-}$ mice. $CCR5^{-/-}$ mice were injected with wild-type mesenchymal cells treated with the inhibitor (CTT) or control peptide (STT). Twenty-four hours later, 7.5×10^5 melanoma cells were injected via the tail vein. Metastases in these groups were compared to $CCR5^{-/-}$ mice injected with $CCR5^{-/-}$ mesenchymal cells. Two weeks after tumor injection the numbers of metastases were counted. **D:** Photomicrographs of a sample of $CCR5^{-/-}$ lungs used in **C**.

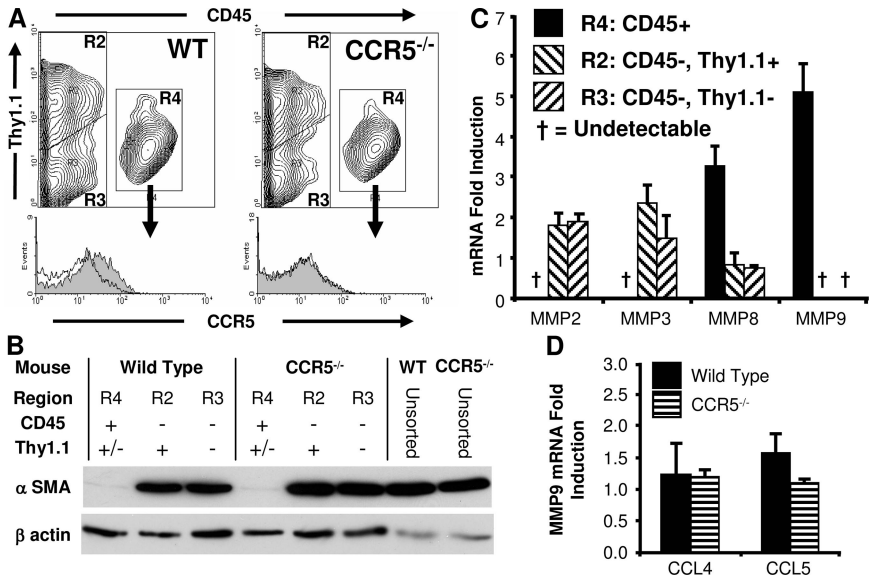

Figure 5. Wild-type pulmonary fibrocytes promote metastasis in CCR5$^{-/-}$ lungs. **A:** Wild-type fibrocytes express CCR5. Representative histograms for CCR5 gated on CD45^{+} mesenchymal cells. Isotype control is shown as the unfilled contour ($n = 6$). **B:** Wild-type and CCR5$^{-/-}$ fibrocytes do not express α-SMA. A representative Western blot showing expression of α-SMA in the CD45^{-} fraction of the mesenchymal cells but not in the CD45^{+} fraction (fibrocytes) ($n = 3$). **C:** Wild-type pulmonary fibrocytes express MMP8 and MMP9. mRNA was harvested from wild-type pulmonary mesenchymal cells sorted by CD45 and Thy1.1. Real-time RT-PCR was used to measure the ratio of MMP transcripts in the sorted population compared with unsorted cells. The graph depicts the mean of four experiments. **D:** Pulmonary mesenchymal cells do not increase MMP9 in response to CCL4 or CCL5. Wild-type and CCR5$^{-/-}$ mesenchymal cells were cultured in serum-free conditions overnight. The following day CCL4 (50 ng/ml), CCL5 (5 ng/ml), or no chemokine (control) was added. mRNA was harvested 6 hours later. Real-time RT-PCR was used to measure a ratio of MMP9 transcripts in the chemokine-treated cells versus the untreated cells. Copy number was normalized to mRNA amount. The graph depicts the mean of these ratios ($n = 6$).

wild-type mesenchymal cells. Analysis of EGFP-Tg wild-type cells demonstrated the viability of these cells at the time of hematogenous seeding of tumor cells. Furthermore, we have shown that the wild-type cells both express CCR5 and respond to CCR5 ligands and that this expression is required for entry into the lung. We also showed that CCR5 was expressed only in the CD45^{+}, CD13^{+} subpopulation of the mesenchymal cells. Because the cells of this subpopulation are referred to as fibrocytes,[25,26] we concluded that fibrocytes contribute to the premetastatic niche.

The capacity of the fibrocyte to increase metastasis was established using injections of only 60,000 CD45^{+} cells. This profound effect on metastasis is best explained by the ability of the fibrocyte to induce MMP9 in the host tissue. One explanation for the induction of MMP9 is that fibrocytes facilitate the invasion of other MMP9-expressing cells. For example, MMP9 on the fibrocyte can activate the chemotactic factors S100A8 and S100A9.[27] These proteins are induced within the premetastatic niche by the distant tumor[28] and can enhance the influx of monocytes. MMP9 also releases vascular endothelial growth factor (VEGF),[29] which may act on bone marrow-derived hematopoietic progenitor cells drawn into the premetastatic niche.[2,3] Monocytes[30] and VEGF receptor^{+} hematopoietic progenitor cells[31] can increase expression of MMP9. Furthermore, fibrocytes may directly increase MMP9 by the production of fibroblast growth factor-1[32] and hepatocyte growth factor.[33]

Our study offers further evidence for the importance of MMP9 in the premetastatic stages of metastasis.[34] MMP9 may precondition the stroma by activating transforming growth factor (TGF)-β.[35] In the later stages of cancer, this cytokine can support tumor progression by promoting angiogenesis and inhibiting immune surveillance.[36] However, in the premetastatic setting, TGF-β's effects are likely on the stroma. Specifically, TGF-β can transform fibrocytes,[37] fibroblasts,[38] and even alveolar epithelial cells,[39] into α-SMA-expressing myofibroblasts. More direct evidence linking MMP9 to the formation of myofibroblasts has been seen in models of lung[33] and liver fibrosis.[40] Whether MMP9 works directly or indirectly, myofibroblasts have been associated with cancer growth[41] and a poorer prognosis.[18]

This study does raise questions about the origin of our injected fibrocytes. Earlier definitions of fibrocytes included bone marrow-derived cells[42] that expressed CoII, CD11b, CD13, CD34, CD45, MHC class II, and CD86.[43] Later definitions recognized that many of these markers may be down-regulated.[37,44] Thus, our CD45^{+}, CD13^{+}, CCR5^{+}, αSMA^{-} cells are consistent with fibrocytes. However, we have previously shown that the transfer of wild-type bone marrow into CCR5$^{-/-}$ mice does not promote metastasis.[8] This result would suggest that these fibrocytes are not bone marrow-derived.

One explanation is that these pulmonary fibrocytes are distinct from bone marrow fibrocytes. In this model, the pulmonary fibrocytes are present at the inception of metastasis and decline throughout the first 5 days. In contrast, bone marrow-derived fibrocytes increase throughout time.[45] These cells are recruited not via CCR5 but by CXCR4 and CCR7.[43] In fact, this recruitment may be the result of CXCL12 production by the resident fibroblasts.[46] These observations would suggest two separate stromal cells axes: resident fibrocytes that facilitate invasion and depend on inflammatory chemokines and recruited fibrocytes that promote growth of established disease and depend on constitutive chemokines. The alternative explanation for the failure of wild-type bone marrow to increase metastasis in CCR5$^{-/-}$ mice is attributable to the radioresistant nature of resident fibrocytes and the slow accumulation of these cells in host tissues after transplant. In this model, the prometastatic effects of fibrocytes are more evident after the direct inoculation of these cells.

Several mouse studies have used bone marrow transplant techniques to demonstrate the dependence of fibrocytes on various chemokine receptors. For example, fibrocytes require CCR1 in wound healing[43] and renal fibrosis,[47] CCR2 in pulmonary fibrosis,[25] CCL3/CCR5

Table 3. Pulmonary Chemokine Expression: Before and After LPS Stimulation

Chemokine	Receptor	Control*	SEM	LPS stimulated	SEM	Fold change†
CXCL15	CXCR5	5.09	0.212	4.70	0.153	
CCL6	**CCR1**	1.63	0.056	1.61	0.110	
CCL21	**CCR7**	0.73	0.042	0.58	0.026	
CXCL7	**CXCR1**, CXCR2	0.58	0.108	0.94	0.207	
CXCL4	**CXCR3**	0.50	0.057	0.63	0.087	
CCL5	**CCR1, CCR5**	0.43	0.042	1.13	0.060	2.7 ± 0.4
CXCL12	**CXCR4**	0.42	0.010	0.33	0.015	
CCL9	**CCR1**	0.33	0.093	0.97	0.086	
CXCL14		0.28	0.026	0.30	0.036	
CXCL16	**CXCR1**, CXCR2	0.28	0.018	0.42	0.017	1.5 ± 0.2
CCL19	**CCR7**	0.22	0.011	0.57	0.043	2.6 ± 0.3
CCL17	**CCR4**	0.22	0.061	0.73	0.041	3.3 ± 1.2
CCL8	**CCR2**, **CCR5**	0.22	0.054	0.19	0.005	
CCL4	**CCR5**	0.21	0.010	0.52	0.040	2.4 ± 0.3
CXCL10	**CXCR3**	0.21	0.103	3.25	0.238	15.3 ± 5.6
CCL20	CCR6	0.17	0.020	0.53	0.036	3.1 ± 0.6
CXCL13	CXCR5	0.16	0.021	0.34	0.038	
CXCL1	CXCR2	0.15	0.035	1.47	0.122	9.7 ± 3.2
CX3CL1	CX3CR	0.13	0.005	0.14	0.005	
CCL24	**CCR3**	0.13	0.005	0.13	0.020	
CCL22	**CCR4**	0.11	0.051	0.28	0.027	2.5 ± 0.1
CXCL9	**CXCR3**	0.11	0.014	0.24	0.031	
CCL2	**CCR2**	0.10	0.015	0.29	0.092	2.8 ± 1.5
CXCL2	CXCR2	0.08	0.001	1.25	0.001	16.2 ± 4.5
CCL28	**CCR3**, CCR10	0.07	0.008	0.07	0.033	
CCL3	**CCR1**, **CCR5**	0.05	0.006	0.37	0.007	6.8 ± 1.6
CCL7	**CCR1, CCR3**, **CCR5**	0.05	0.006	0.09	0.005	
CCL12	**CCR2**	0.04	0.001	0.08	0.007	
CCL11	**CCR3**	0.04	0.001	0.08	0.001	
CCL25	**CCR9**	0.03	0.001	0.03	0.001	
CXCL11	**CXCR3**	0.02	0.003	0.03	0.021	
CXCL5	CXCR2	0.02	0.002	0.15	0.034	

Bold: chemokine receptors associated with fibrocytes[44]; underlined: expressed chemokines.
*Affymetrix array raw expression data normalized to a set of index genes.
†$P < 0.002$ (fold change is only given for statistically significant increases).

in bleomycin-induced lung injury,[48] and CCL21/CCR7 in idiopathic interstitial pneumonia[34] and renal fibrosis.[49] In all of these studies, chemokines are induced by a stimulus (eg, wounding, bleomycin, uretral obstruction, and so forth). Although baseline expression of the CCR5 ligands is adequate to establish wild-type fibrocytes in the lungs of wild-type and $CCR5^{-/-}$ mice, it does not lead to a dramatic turnover in pulmonary fibrocytes after syngeneic transplant. Hence, fibrocyte populations are more reflective of the host than the donor mice.

If the induction of MMP9 by $CCR5^{+}$ fibrocytes is the reason that wild-type mice develop more metastases

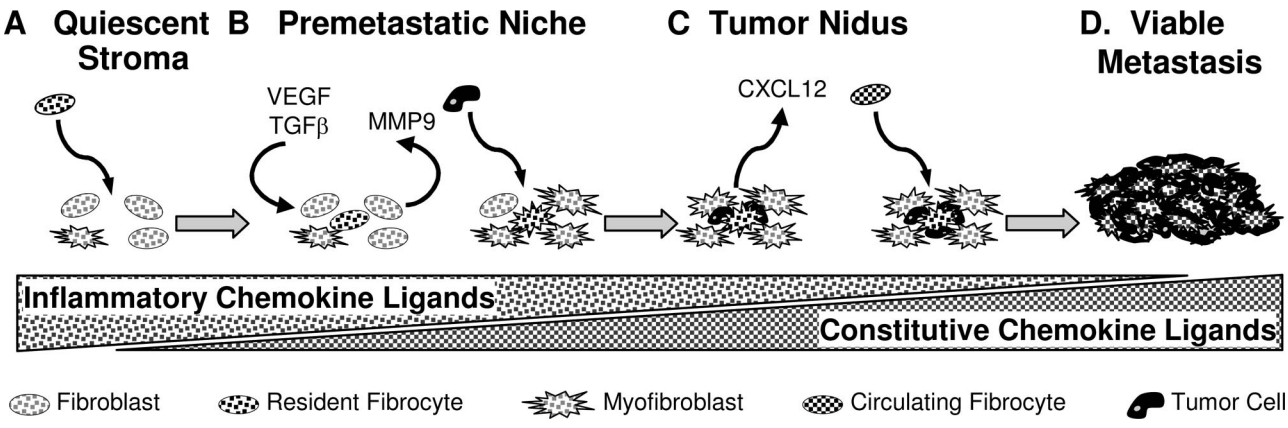

Figure 6. A model for the role of inflammatory and constitutive chemokines in metastasis. **A:** The quiescent stroma begins with a low risk for accommodating metastasis. Pulmonary fibrocytes enter this area in a process facilitated by CCR5. The migration of fibrocytes may be further enhanced by inflammation or by changes induced by the distant tumor. **B:** Pulmonary fibrocytes induce the expression of MMP9. This metalloproteinase can support the developing premetastatic niche by promoting the expression and activation of VEGF and TGF-β. TGF-β will further advance this niche by the conversion of fibroblasts into myofibroblasts. Eventually, this niche becomes vulnerable to invasion by circulating tumor cells. **C:** Entering tumor cells interact with the resident stroma to produce constitutive chemokines such as CXCL12. This signal promotes the influx of circulating fibrocytes via CCR7. These cells become incorporated into the tumor and produce factors that promote the growth of the tumor nidus. **D:** The process continues resulting in a metastatic tumor.

than CCR5$^{-/-}$ mice, one would expect wild-type mice to have higher baseline levels of MMP9 expression. However, MMP9 levels are not significantly different between the two strains (data not shown). One possible explanation for this apparent discrepancy is the inability of real-time PCR to detect small, loco-regional differences. A small increase in MMP9 may have a profound effect on metastasis because several positive feedback loops exist to amplify its effects. Alternatively, injection of wild-type fibrocytes may overcome another anti-metastatic effect found in the stroma of CCR5$^{-/-}$ mice. In either case, our results support the conclusion that wild-type fibrocytes are more efficient in establishing a premetastatic niche than CCR5$^{-/-}$ fibrocytes.

Our results can be synthesized with the results of others using the model illustrated in Figure 6. Small numbers of pulmonary fibrocytes enter the host tissue. This process is facilitated by CCR5 and may be accelerated in the setting of inflammation. After invasion, the fibrocytes contribute to the premetastatic niche through the induction of MMP9 and the expression of fibronectin. MMP9 expression leads to the releases of VEGF and activation of TGF-β, which transforms resident fibroblasts into myofibroblasts. In this environment, tumor cells are able to invade and thrive. After the invasion of cancer cells, chemotactic factors are produced by the interaction of tumor cells and stroma. These chemokines lead to the recruitment of other fibrocytes. These fibrocytes become activated and begin producing factors that support the growth of the tumor nidus. The process continues and a life-threatening metastasis is formed.

References

1. Poste G, Paruch L: Stephen Paget MD, F.R.C.S., (1855–1926). A retrospective. Cancer Metastasis Rev 1989, 8:i-97
2. Kaplan RN, Rafii S, Lyden D: Preparing the "soil": the premetastatic niche. Cancer Res 2006, 66:11089–11093
3. Kaplan RN, Riba RD, Zacharoulis S, Bramley AH, Vincent L, Costa C, MacDonald DD, Jin DK, Shido K, Kerns SA, Zhu Z, Hicklin D, Wu Y, Port JL, Altorki N, Port ER, Ruggero D, Shmelkov SV, Jensen KK, Rafii S, Lyden D: VEGFR1-positive haematopoietic bone marrow progenitors initiate the pre-metastatic niche. Nature 2005, 438:820–827
4. Zlotnik A, Yoshie O: Chemokines: a new classification system and their role in immunity. Immunity 2000, 12:121–127
5. Sallusto F, Mackay CR, Lanzavecchia A: The role of chemokine receptors in primary, effector, and memory immune responses. Annu Rev Immunol 2000, 18:593–620
6. Horuk R: Chemokine receptors. Cytokine Growth Factor Rev 2001, 12:313–335
7. Moser B, Willimann K: Chemokines: role in inflammation and immune surveillance. Ann Rheum Dis 2004, 63:ii84–ii89
8. van Deventer HW, O'Connor W Jr, Brickey WJ, Aris RM, Ting JP, Serody JS: C-C chemokine receptor 5 on stromal cells promotes pulmonary metastasis. Cancer Res 2005, 65:3374–3379
9. Andres PG, Beck PL, Mizoguchi E, Mizoguchi A, Bhan AK, Dawson T, Kuziel WA, Maeda N, MacDermott RP, Podolsky DK, Reinecker HC: Mice with a selective deletion of the CC chemokine receptors 5 or 2 are protected from dextran sodium sulfate-mediated colitis: lack of CC chemokine receptor 5 expression results in a NK1.1+ lymphocyte-associated Th2-type immune response in the intestine. J Immunol 2000, 164:6303–6312
10. Kuziel WA, Dawson TC, Quinones M, Garavito E, Chenaux G, Ahuja SS, Reddick RL, Maeda N: CCR5 deficiency is not protective in the early stages of atherogenesis in apoE knockout mice. Atherosclerosis 2003, 167:25–32
11. Serody JS, Burkett SE, Panoskaltsis-Mortari A, Ng-Cashin J, McMahon E, Matsushima GK, Lira SA, Cook DN, Blazar BR: T-lymphocyte production of macrophage inflammatory protein-1alpha is critical to the recruitment of CD8(+) T cells to the liver, lung, and spleen during graft-versus-host disease. Blood 2000, 96:2973–2980
12. Schüler T, Kornig S, Blankenstein T: Tumor rejection by modulation of tumor stromal fibroblasts. J Exp Med 2003, 198:1487–1493
13. Bergstralh DT, Taxman DJ, Chou TC, Danishefsky SJ, Ting JP: A comparison of signaling activities induced by Taxol and desoxyepothilone B. J Chemother 2004, 16:563–576
14. Wexler H, Orme SK, Ketcham AS: Biological behavior through successive transplant generations of transplantable tumors derived originally from primary chemically induced and spontaneous sources in mice. J Natl Cancer Inst 1968, 40:513–523
15. Altemeier WA, Matute-Bello G, Gharib SA, Glenny RW, Martin TR, Liles WC: Modulation of lipopolysaccharide-induced gene transcription and promotion of lung injury by mechanical ventilation. J Immunol 2005, 175:3369–3376
16. Hammer O, Harper DAT, Ryan PD: Palaeontological statistics software package for education and data analysis. Palaeontologia Electronica 2001, 4:9
17. Phipps RP, Penney DP, Keng P, Quill H, Paxhia A, Derdak S, Felch ME: Characterization of two major populations of lung fibroblasts: distinguishing morphology and discordant display of Thy 1 and class II MHC. Am J Respir Cell Mol Biol 1989, 1:65–74
18. Tsujino T, Seshimo I, Yamamoto H, Ngan CY, Ezumi K, Takemasa I, Ikeda M, Sekimoto M, Matsuura N, Monden M: Stromal myofibroblasts predict disease recurrence for colorectal cancer. Clin Cancer Res 2007, 13:2082–2090
19. Surowiak P, Suchocki S, Gyorffy B, Gansukh T, Wojnar A, Maciejczyk A, Pudelko M, Zabel M: Stromal myofibroblasts in breast cancer: relations between their occurrence, tumor grade and expression of some tumour markers. Folia Histochem Cytobiol 2006, 44:111–116
20. Del Corno M, Liu QH, Schols D, de Clercq E, Gessani S, Freedman BD, Collman RG: HIV-1 gp120 and chemokine activation of Pyk2 and mitogen-activated protein kinases in primary macrophages mediated by calcium-dependent, pertussis toxin-insensitive chemokine receptor signaling. Blood 2001, 98:2909–2916
21. Ma B, Kang MJ, Lee CG, Chapoval S, Liu W, Chen Q, Coyle AJ, Lora JM, Picarella D, Homer RJ, Elias JA: Role of CCR5 in IFN-gamma-induced and cigarette smoke-induced emphysema. J Clin Invest 2005, 115:3460–3472
22. Nikkola J, Vihinen P, Vuoristo M-S, Kellokumpu-Lehtinen P, Kahari V-M, Pyrhonen S: High serum levels of matrix metalloproteinase-9 and matrix metalloproteinase-1 are associated with rapid progression in patients with metastatic melanoma. Clin Cancer Res 2005, 11:5158–5166
23. Kolaczkowska E, Chadzinska M, Scislowska-Czarnecka A, Plytycz B, Opdenakker G, Arnold B: Gelatinase B/matrix metalloproteinase-9 contributes to cellular infiltration in a murine model of zymosan peritonitis. Immunobiology 2006, 211:137–148
24. Medina OP, Soderlund T, Laakkonen LJ, Tuominen EKJ, Koivunen E, Kinnunen PKJ: Binding of novel peptide inhibitors of type IV collagenases to phospholipid membranes and use in liposome targeting to tumor cells in vitro. Cancer Res 2001, 61:3978–3985
25. Moore BB, Kolodsick JE, Thannickal VJ, Cooke K, Moore TA, Hogaboam C, Wilke CA, Toews GB: CCR2-mediated recruitment of fibrocytes to the alveolar space after fibrotic injury. Am J Pathol 2005, 166:675–684
26. Lama VN, Phan SH: The extrapulmonary origin of fibroblasts: stem/progenitor cells and beyond. Proc Am Thorac Soc 2006, 3:373–376
27. Greenlee KJ, Corry DB, Engler DA, Matsunami RK, Tessier P, Cook RG, Werb Z, Kheradmand F: Proteomic identification of in vivo substrates for matrix metalloproteinases 2 and 9 reveals a mechanism for resolution of inflammation. J Immunol 2006, 177:7312–7321
28. Hiratsuka S, Watanabe A, Aburatani H, Maru Y: Tumour-mediated upregulation of chemoattractants and recruitment of myeloid cells predetermines lung metastasis. Nat Cell Biol 2006, 8:1369–1375
29. Bergers G, Brekken R, McMahon G, Vu TH, Itoh T, Tamaki K, Tanzawa K, Thorpe P, Itohara S, Werb Z, Hanahan D: Matrix metalloproteinase-9 triggers the angiogenic switch during carcinogenesis. Nat Cell Biol 2000, 2:737–744
30. Azenshtein E, Luboshits G, Shina S, Neumark E, Shahbazian D, Weil M, Wigler N, Keydar I, Ben-Baruch A: The CC chemokine RANTES in

breast carcinoma progression: regulation of expression and potential mechanisms of promalignant activity. Cancer Res 2002, 62: 1093–1102
31. Hiratsuka S, Nakamura K, Iwai S, Murakami M, Itoh T, Kijima H, Shipley JM, Senior RM, Shibuya M: MMP9 induction by vascular endothelial growth factor receptor-1 is involved in lung-specific metastasis. Cancer Cell 2002, 2:289–300
32. Lungu G, Covaleda L, Mendes O, Martini-Stoica H, Stoica G: FGF-1-induced matrix metalloproteinase-9 expression in breast cancer cells is mediated by increased activities of NF-kB and activating protein-1. Mol Carcinog 2008, 47:424–435
33. Mizuno S, Matsumoto K, Li MY, Nakamura T: HGF reduces advancing lung fibrosis in mice: a potential role for MMP-dependent myofibroblast apoptosis. FASEB J 2005, 19:580–582
34. Nicoud IB, Jones CM, Pierce JM, Earl TM, Matrisian LM, Chari RS, Gorden DL: Warm hepatic ischemia-reperfusion promotes growth of colorectal carcinoma micrometastases in mouse liver via matrix metalloproteinase-9 induction. Cancer Res 2007, 67:2720–2728
35. Stover DG, Bierie B, Moses HL: A delicate balance: TGF-β and the tumor microenvironment. J Cell Biochem 2007, 101:851–861
36. Jakowlew S: Transforming growth factor-β in cancer and metastasis. Cancer Metastasis Rev 2006, 25:435–457
37. Schmidt M, Sun G, Stacey MA, Mori L, Mattoli S: Identification of circulating fibrocytes as precursors of bronchial myofibroblasts in asthma. J Immunol 2003, 171:380–389
38. Thannickal VJ, Lee DY, White ES, Cui Z, Larios JM, Chacon R, Horowitz JC, Day RM, Thomas PE: Myofibroblast differentiation by transforming growth factor-beta 1 is dependent on cell adhesion and integrin signaling via focal adhesion kinase. J Biol Chem 2003, 278:12384–12389
39. Willis BC, Liebler JM, Luby-Phelps K, Nicholson AG, Crandall ED, du Bois RM, Borok Z: Induction of epithelial-mesenchymal transition in alveolar epithelial cells by transforming growth factor-{beta}1: potential role in idiopathic pulmonary fibrosis. Am J Pathol 2005, 166:1321–1332
40. Roderfeld M, Weiskirchen R, Wagner S, Berres M-L, Henkel C, Grotzinger J, Gressner AM, Matern S, Roeb E: Inhibition of hepatic fibrogenesis by matrix metalloproteinase-9 mutants in mice. FASEB J 2006, 20:444–454
41. Micke P, Ostman A: Tumour-stroma interaction: cancer-associated fibroblasts as novel targets in anti-cancer therapy? Lung Cancer 2004, 45(Suppl 2):S163–S175
42. Ishii G, Sangai T, Sugiyama K, Ito T, Hasebe T, Endoh Y, Magae J, Ochiai A: In vivo characterization of bone marrow-derived fibroblasts recruited into fibrotic lesions. Stem Cells 2005, 23:699–706
43. Abe R, Donnelly SC, Peng T, Bucala R, Metz CN: Peripheral blood fibrocytes: differentiation pathway and migration to wound sites. J Immunol 2001, 166:7556–7562
44. Bellini A, Mattoli S: The role of the fibrocyte, a bone marrow-derived mesenchymal progenitor, in reactive and reparative fibroses. Lab Invest 2007, 87:858–870
45. Ishii G, Sangai T, Oda T, Aoyagi Y, Hasebe T, Kanomata N, Endoh Y, Okumura C, Okuhara Y, Magae J, Emura M, Ochiya T, Ochiai A: Bone-marrow-derived myofibroblasts contribute to the cancer-induced stromal reaction. Biochem Biophys Res Commun 2003, 309:232–240
46. Orimo A, Gupta PB, Sgroi DC, Arenzana-Seisdedos F, Delaunay T, Naeem R, Carey VJ, Richardson AL, Weinberg RA: Stromal fibroblasts present in invasive human breast carcinomas promote tumor growth and angiogenesis through elevated SDF-1/CXCL12 secretion. Cell 2005, 121:335–348
47. Eis V, Luckow B, Vielhauer V, Siveke JT, Linde Y, Segerer S, de Lema GP, Cohen CD, Kretzler M, Mack M, Horuk R, Murphy PM, Gao J-L, Hudkins KL, Alpers CE, Grone H-J, Schlondorff D, Anders H-J: Chemokine receptor CCR1 but not CCR5 mediates leukocyte recruitment and subsequent renal fibrosis after unilateral ureteral obstruction. J Am Soc Nephrol 2004, 15:337–347
48. Ishida Y, Kimura A, Kondo T, Hayashi T, Ueno M, Takakura N, Matsushima K, Mukaida N: Essential roles of the CC chemokine ligand 3-CC chemokine receptor 5 axis in bleomycin-induced pulmonary fibrosis through regulation of macrophage and fibrocyte infiltration. Am J Pathol 2007, 170:843–854
49. Sakai N, Wada T, Yokoyama H, Lipp M, Ueha S, Matsushima K, Kaneko S: Secondary lymphoid tissue chemokine (SLC/CCL21)/CCR7 signaling regulates fibrocytes in renal fibrosis. Proc Natl Acad Sci USA 2006, 103:14098–14103